Physica A 451 (2016) 578–591

Contents lists available at ScienceDirect

Physica A

journal homepage: www.elsevier.com/locate/physa

Optimization strategy for and structural properties of traffic efficiency under bounded information accessibility

Ahn Sanghyun *, Ha Seungwoong [1], Soo Yong Kim

Department of Physics, Korea Advanced Institute of Science and Technology, Daejeon 305-701, Republic of Korea

HIGHLIGHTS

- We introduce a new model which is more sensitive to the reality than previous models.
- We propose two main factors for traffic efficiency, section area and symmetricity.
- We find the optimal point for traffic efficiency, which causes the phase transition.
- We find the optimal structure for traffic under bounded information accessibility.
- We carry out investigation into empirical study for credibility of our numerical simulation.

ARTICLE INFO

Article history:
Received 27 August 2015
Received in revised form 7 December 2015
Available online 9 February 2016

Keywords:
Bounded information
Algorithm
Optimization of traffic system
Section area
Symmetricity

ABSTRACT

A vital challenge for many socioeconomic systems is determining the optimum use of limited information. Traffic systems, wherein the range of resources is limited, are a particularly good example of this challenge. Based on bounded information accessibility in terms of, for example, high costs or technical limitations, we develop a new optimization strategy to improve the efficiency of a traffic system with signals and intersections. Numerous studies, including the study by Chowdery and Schadschneider (whose method we denote by ChSch), have attempted to achieve the maximum vehicle speed or the minimum wait time for a given traffic condition. In this paper, we introduce a modified version of ChSch with an independently functioning, decentralized control system. With the new model, we determine the optimization strategy under bounded information accessibility, which proves the existence of an optimal point for phase transitions in the system. The paper also provides insight that can be applied by traffic engineers to create more efficient traffic systems by analyzing the area and symmetry of local sites. We support our results with a statistical analysis using empirical traffic data from Seoul, Korea.

1. Introduction

Traffic flows represent various and intriguing complex phenomena. Numerous studies of traffic system problems have motivated research by physicists due to their statistical and dynamical features [1–11]. Due to the inherent properties of a traffic system, an agent-based model (ABM) has been employed to study traffic dynamics. We can classify a traffic system with an ABM into two categories for study: pedestrian dynamics and vehicle dynamics. Pedestrian problems have been investigated with microscopic models, including the cellular automata (CA) model [10–16], the social force model [5,17,18],

* Corresponding author.
E-mail address: nicehyun@kaist.ac.kr (A. Sanghyun).

[1] Equally contributed.

http://dx.doi.org/10.1016/j.physa.2015.12.165
0378-4371/

the magnetic force model [19] and the centrifugal force model [6]. In contrast to pedestrian problems, vehicle problems focus not only on individual behavior but also on the structural effect of important variables. The traffic signal is one of the most important variables for describing a phase transition, such as the transition from the jam phase to the free-flow phase [7,20,21]. Although numerous studies about traffic jams, chaotic traffic flows, pedestrian flows, and the sequence of traffic signals have been performed [22–27], few studies have addressed system efficiency. System efficiency is defined as the ratio of the increase in traffic flow to the cost of using traffic signals to create more efficient traffic conditions in an urban traffic system. The control of efficient traffic signals is important for improving mobility and reducing the wait time of vehicles on the road because intersections are the most common reason for speed reductions in a large city [28]. The jam state of a traffic system increases the wait time or reduces vehicle speeds. To mitigate the jam state, various studies have been intensively performed in many disciplines, and brilliant mathematical and numerical models have been introduced.

We discuss the ChSch model because it is the simplest toy model available for developing the decentralized control concept with as few variables as possible. Previous studies have examined decentralized and self-organized traffic signal control [7,29]. However, we focus on an independently functioning decentralized control system to determine the association between the real world and the numerical model using a simplified toy model. Although most parameters vary, we select identical values for all vehicles to minimize the number of parameters, facilitate calibration, achieve robustness and exclude irregular results due to parameter variations. We ensure that this approach simplifies the model for use in various studies.

The ChSch model simulates urban traffic with intersections [30,31]. The model combines two previously suggested models the Biham–Middleton–Levin (BML) model [24,32] and the Nagel–Schreckenberg (NaSch) model [33,34]; two-dimensional space is extracted from the BML model, and traffic signals are extracted from the NaSch model. This combination produces a realistic traffic model with two major factors concerning traffic jams: the movements of vehicles and the control of traffic signals. Brockfeld and Barlovic [1] investigated the nature of the modified ChSch model using several global traffic strategies and concluded that a rule named the Green Wave Strategy (GWS) outperforms other strategies for both low and high vehicle densities. The GWS has an offset parameter, with which the switching time of adjacent traffic signals is delayed. The majority of these studies have attempted to improve traffic conditions in regard to the mean flow, which is the average distance for the movement of all vehicles. All variables, such as traffic signals, movement of vehicles and density of vehicles, control the traffic phase from the jam phase to the free-flow phase or vice versa. The strategy can enhance traffic conditions via other approaches [35,36]. The GWS is the best strategy, because it incorporates all information on a simulation map, which results in high costs and inefficient in use.

In this paper, we focus on the bounded range of information to control a traffic signal system by considering the related high costs and technical limitations. This method exhibits more affinity with real traffic conditions because districts independently manage pedestrians and vehicles in actual urban traffic situations [37–39]. If information is limited in a traffic system, namely by the restriction of the interlocking range of traffic signals, the efficiency of a traffic system will vary based on the information range. Considering limitations on actual information about an urban traffic system caused by technical issues, we analyze the effect of limited information to obtain a meaningful solution. The limited information causes the entire map to be partitioned into various independent divisions. Each division is physically connected; however, independent players are functionally considered. In addition, the area and symmetry when the system is divided into small lots is considered. Thus, we investigate not only the amount of information compared to the size of each section area but also the effect of the rectangular symmetry of the local site. We determine if two parameters can fulfill their roles as valuable components that are properly based on the empirical data of Seoul, which is also known as the capital city of South Korea.

This paper is organized as follows: In the following section, the definition, characteristics and regulation of the model used in the simulation are presented. We attempt to modify the ChSch model to prevent gridlock of vehicles as presented by Ref. [30] and introduce several parameters to assess the nature of our model. In Section 3, the mean flow (equivalent to the concept of velocity flow), which is introduced under various limited information circumstances, is tested via numerical simulation. The results with the alteration of several parameters and the interpretation of the simulations are presented. A newly defined symmetricity is proposed to test the role of symmetry in traffic efficiency. We provide a comparison between the numerical simulation data and the empirical data. Section 4 presents a discussion of the obtained results and of the highlights of the study.

2. Models and strategies

2.1. Model settlement

The ChSch model reflects two critical features of actual urban traffic: numerous vehicles and traffic signals [30]. The entire map is composed of $N \times N$ intersections connected by streets with a length L, including traffic signals; thus, $L - 1$ cells represent single streets. Fig. 1 shows a snapshot of our simulation model. Every street consists of a set of cells that forms a square lattice. The total number of cells for each successive street is $L_T = NL$. After establishing the map with intersections and traffic signals, vehicles are randomly scattered with a given density ρ. The ChSch model contains only two direction-bound vehicles; the number of eastbound vehicles and northbound vehicles are identical. A periodic boundary condition is applied to conserve the number and directions of the vehicles. The total number of vehicles in the entire map

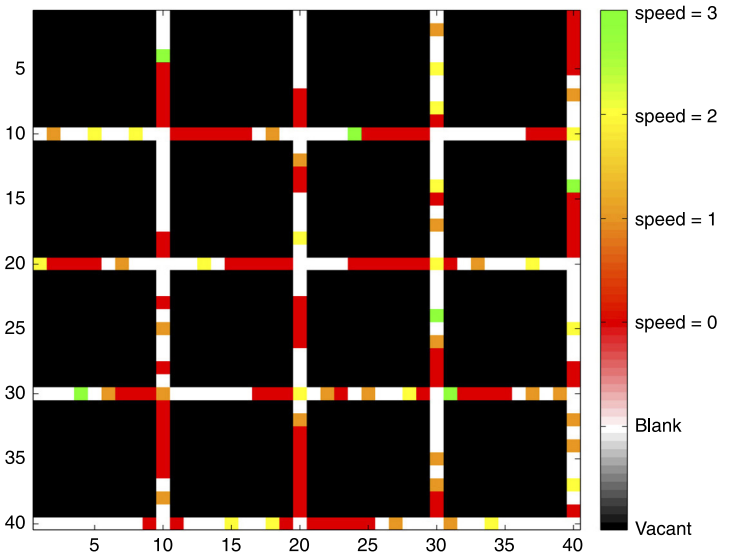

Fig. 1. Snapshot of 4×4 ChSch model with density 0.5. The distance between two intersections is $L - 1 = 9$. Black cells are vacant, white cells represent street cells without cars, and other colors represent speed of vehicles on the street. (For interpretation of the references to color in this figure legend, the reader is referred to the web version of this article.)

is $N_v = 2N_{east} = 2N_{south}$, and the vehicle density ρ is defined by

$$\rho = \frac{N_v}{N^2(2L-1)}. \tag{1}$$

The vehicles can switch their velocities according to the NaSch model, in which the range of velocities is an integer from 0 to $v_{\max}$, where $v_{\max}$ is a given maximum speed (refer to Appendix A for details of the model). The modification of the ChSch model protects the simulation from a completely blocked state, which we refer to as gridlock; gridlock is an obstacle to the exploration of high-density cases. The ChSch model, which reproduces all observed collective effects of vehicle flow, uses all interactions over the entire map. In contrast, the interactions are local in our approach.

2.2. Description of strategies

We form an $N \times N$ lattice with east streets and north streets. The lattice is mapped using rectangular coordinates, in which each traffic signal is assigned to a grid point of the coordinate system. According to the GWS, a traffic signals delay time T_{delay} is given. T_{delay} is the time delay between two traffic signal phases, i.e., green and red. If we denote traffic cycle time T as a time interval to change traffic light, one color to another, a traffic signal with the coordinate (i, j) has the offset parameter $\Delta T_{i,j}$, for $i, j = 0, 1, \ldots, N$, which is given by following equation with cycle time T of flipping traffic light.

$$\Delta T_{i,j} = [(i+j)T_{delay}] \bmod (2T), \quad (i, j = 0, 1, \ldots, N-1). \tag{2}$$

The offset parameter determines the delay time for each traffic signal. Fig. 2(a) shows the phase change diagram of the traffic signals over time. As its name implies, the GWS propagates a wave of green signal time to maintain the speeds of vehicles without braking.

In this paper, we propose the process of bounded information accessibility to develop an analogy with real world traffic systems. Our suggestion reflects an information restriction that is based on the notion that every traffic system can manage an entire range of signals to simultaneously interlock every intersection [37,40]. To describe the information restriction in the traffic system, we introduce divided GWS (D-GWS). This strategy is considered to be a type of decentralized control system with independently divided sections. The D-GWS regulates the coupled range of the GWS from the entire map to specific rectangular divisions, which facilitates the role of each section as an independent local system; thus, the entire map is composed of numerous independent divisions. This local effect can have an enormous influence on macroscopic quantities, such as flow and wait time. If we attempt to divide the entire map into $x \times y$ independent rectangular divisions, we obtain $N_x \times N_y$ divisions, where $N_x = N/x$, $N_y = N/y$, and x and y are divisors of N. Then, we independently apply the GWS to each division. This procedure is expressed by D-GWS(x, y); for example, 8×8 D-GWS(2, 4) indicates that the 8×8 ChSch model is divided into a series of 2×4 rectangular divisions, and each section is independently governed by the GWS (refer to Fig. 2(b)). One of the 8×8 D-GWS extreme cases is the 8×8 D-GWS(8, 8), which exhibits the same behavior as the 8×8 GWS. From Appendix B, we see that the extreme cases of our model yield results that are similar to the results of the previous GWS study [1].

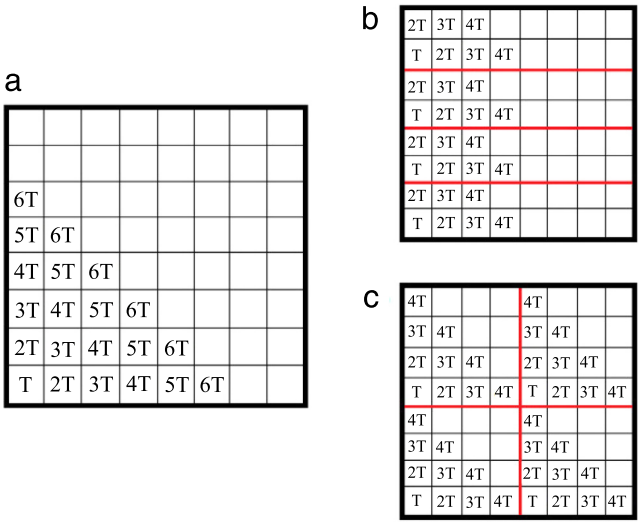

Fig. 2. (a) Diagram of normal 8 × 8 GWS, (b) and (c) are examples of 8 × 8 D-GWS, D-GWS(2, 4) and G-GWS(4, 4), respectably. The D-GWS applies GWS to each section independent, thus there are individual starting points for each section. The red line is taken to be the boundary of each section. T in diagram denotes the cycle time, namely offset parameter T_{delay}. The character in each cell represents when the light goes green. (For interpretation of the references to color in this figure legend, the reader is referred to the web version of this article.)

Throughout this paper, we identify rectangular divisions, which can completely cover the entire map. The width and height of each section should be one of the divisors of N. For the $N \times N$ ChSch model, $d(n)(d(n)+1)/2$ section types are possible, where $d(n)$ denotes the number of divisors of N. By definition, $N \times N$ D-GWS(N, N) is identical to $N \times N$ GWS and $N \times N$ D-GWS(1,1), which gives a perfectly synchronized state with $N = 1$ or a random state. Compared with the GWS, some vehicles have to stop between sections that are independently controlled, which suggests that a vehicle would be blocked when the vehicle progresses to another section because the individual sections cannot work together. We refer to this phenomenon as a phase gap in the D-GWS. Clearly, the D-GWS is less efficient than the GWS, which is represented by the mean flow. Therefore, the area of the section should be proportional to the efficiency because the D-GWS with a large section has a less effective phase gap, which can cause a decrement in efficiency. Because the section area is an important factor in terms of traffic efficiency, we can conjecture that a critical point of the traffic efficiency exists in regard to the section area that depicts the phase transition. We can also explore the case in which the section areas are similar but have different widths and heights. To investigate in more detail, we define a parameter named the symmetricity S, which is used to compare the efficiency between identical section areas. The symmetricity is the simple ratio between the width and the height for the rotation symmetry of the D-GWS, which is defined by b/a where a and b is a length of shorter side and longer side of rectangular section, respectively. Thus, symmetricity is always greater than or equal to 1. For example, the symmetricity of the D-GWS(3, 27) is 9, same as D-GWS(27, 3). A symmetricity of 1 indicates that the section is a perfect square. Our modified ChSch model is based on plausible interactions; due to its simplicity, it is robust with respect to parameter variations. Therefore, it is suitable for drawing conclusions about the possible mechanics underlying the effects of section area and symmetricity.

3. Simulation results

We set the maximum velocity $v_{\max} = 5$ and the street length $L = 50$. To prevent model artifacts, an arbitrary and small amount of irregularity is needed. This irregularity is introduced by the random parameter $p = 0.1$ for the simulation. Based on these constant variables, the parameters that can affect the mean flow of the system include the density, area of the section, and symmetricity of the section. We use the two density parameters 0.05 and 0.7, which are representative of the free-flow phase and the jam phase, respectively. The meaning of the GWS (and the D-GWS) could not be applied to the system with high density due to a regular jam. However, the GWS shows a significant effect with the proper T_{delay} even in the jam phase from the previous study [1] without departing from the concept of the GWS in the high-density case. The preservation of the concept of the GWS is detailed in Appendix B.

3.1. Fixed symmetricity

We fix the symmetricity of the division with the D-GWS to exclude the influence of symmetricity on the traffic efficiency. The purpose of our study is to determine the relationship between the section area and the variation in the velocity-mean flow D which is substitution for the mean flow J and the critical point, which indicates the phase transition of the system efficiency. First, we introduce the parameter D, which is a rate given by $D = \Delta J/\Delta A$ for each point. Fig. 3 shows both J

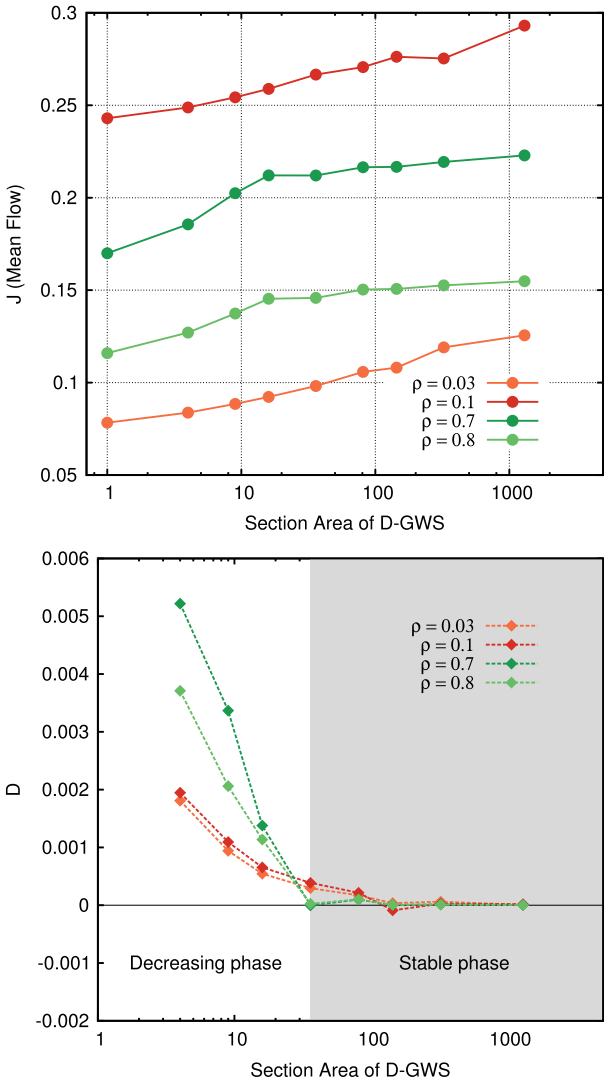

Fig. 3. J (top) and D (bottom) vs. the section area of D-GWS with different vehicle density. The graph shows two similar yet different forms at low and high densities. Low density of D-GWS shows a continuous falling curve ending up with stable state of zero D value. Conversely, high density of the D-GWS divides clearly into two phases, sharply decreasing phase and stable phase with zero point. The results imply that there is a critical point which makes extension of the area meaningless. Mean flow is measured by taking the average of the vehicle velocity delivered by traffic cycle time $T = 1$ to $T = 150$.

and D versus the area of the section in 36×36 D-GWS with four different densities. In the graph, the symmetricity of the four cases is fixed at 1; thus, each of the data points is the J and D value of 36×36 D-GWS(1, 1), 36×36 D-GWS(2, 2), …, 36×36 D-GWS(36, 36). In regard to D, first-order phase transitions occur in the high-density phases; the second-order phase transition represents the mean flow J. We observe that D deceases with an increase in the section area. A specific point exists at which D is maintained near zero after that point. No contribution to the mean flow with an increase in the section area after the critical value is observed because D follows the level of contribution from the extension of the section area. We can also predict and verify the diminishing marginal rate of area extension prior to the critical value. We have conducted the simulation using various densities and achieved similar results with distinguishable high- and low-density cases (we have not shown the other cases). In Fig. 4, we explore the effect of lattice size and the critical point of section area with the symmetricity value $S = 1$. We figure out that section area has a huge contribution to the mean flow, however, section area after the critical point has a tiny contribution to the mean flow. Although we apply various lattice sizes, crossover always occurs at around D-GWS(4, 4).

For further analysis, we only focus on representatives of the free-flow phase and the jam phase with densities of $\rho = 0.05$ and $\rho = 0.7$, respectively. Qualitative differences between the D-GWS for the densities $\rho = 0.05$ and $\rho = 0.7$ are identified. In the early part of the case with $\rho = 0.05$, D is lower and decreases to zero in a smoother manner than in the case of $\rho = 0.7$. The separate phases are relatively distinct for the case of $\rho = 0.7$. The value of D significantly decreases before it reaches a fourth point (D-GWS(4, 4)) and remains nearly zero in the remainder of the range. Recall that D is a unit of the efficiency of

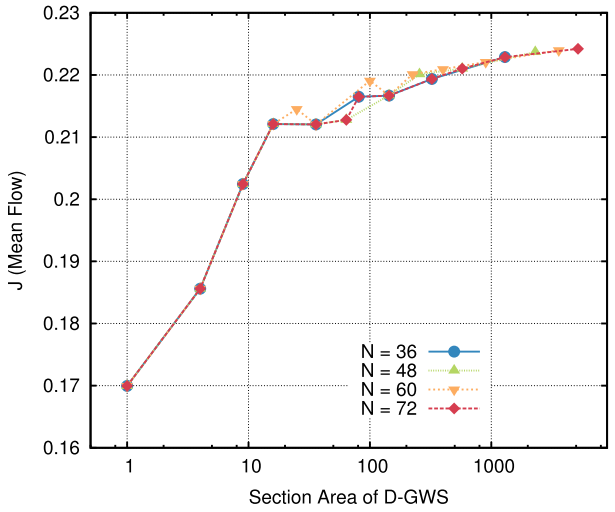

Fig. 4. Mean flow J vs. section area with various lattice size. Section area makes a huge contribution to the mean flow J in earlier part of graph, however, the section area makes a very tiny contribution to the mean flow J in later part of graph, regardless of lattice size. Therefore, the mean flow is plodding along with near flat line growth after the fourth point(D-GWS(4, 4)). We plot the figure based on the map size $N = 36, 48, 60$, and 72 with the fixed symmetricity value $S = 1$, where random parameter $p = 0.1$, the vehicle density $\rho = 0.7$, and offset parameter $T_{delay} = -55$.

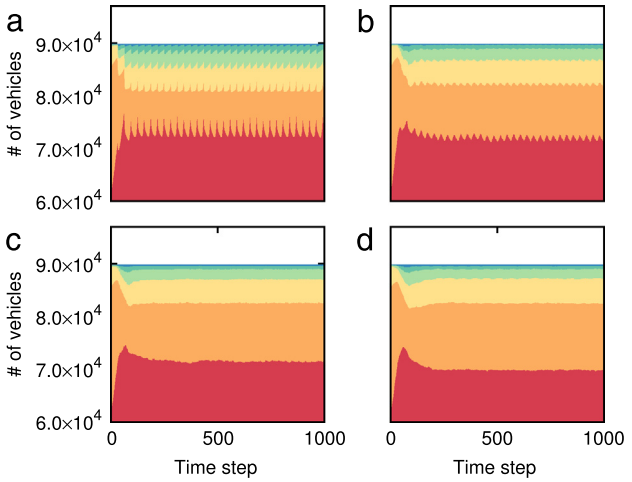

Fig. 5. Vehicle speed histogram of 36×36 D-GWS(c, c) with $\rho = 0.7$ and $T = 50$, where c is (a) 1, (b) 3, (c) 4, and (d) 36. Red, orange, yellow, light green, green, and blue color represents cars in speed 0, 1, 2, 3, 4, and 5, respectively. Total number of the vehicles N_v is 89192. Because all of the D-GWS has more than to 60 thousands vehicles with speed 0, the part of the histogram lower than 6.0×10^5 is leaved out for graph interpretation. We can check the periodic fluctuation induced by T, which yields overall decrease of mean flow. This negative effect is maintained in larger section area, but suddenly vanishes in D-GWS(4, 4). In microscopic view, there is only subtle difference between crossover point D-GWS(4, 4) and full scope D-GWS, D-GWS(36, 36). (For interpretation of the references to color in this figure legend, the reader is referred to the web version of this article.)

the area increment, and D remaining zero suggests no effect of the section area extension. This result implies a difference in the diminishing marginal rate of the area extension between high-density and low-density cases, which is reasonable because no disturbance to other cars occurs in the free-flow phase. The only influence on the effect on deceleration comes from the traffic signals; therefore, the effect of the phase gap among sections becomes a significant factor and requires an external driving force to continuously maintain the relatively high value of D. In the case of the jam phase, the condition of the system is completely different because the vehicle should experience the collision with other vehicles. Due to the congestion, the early stage of the area extension will significantly increase the mean flow in the jam phase, which results in the high value of D. From the D-GWS, we can investigate the relationship between the section area and the traffic efficiency. The result is the critical point whereby the phase transition is produced, in which the area extension cannot serve a large role in terms of increasing efficiency.

From Fig. 4, D-GWS(4, 4) point is critical point, which means that the mean flow phase over section area shifts from increasing state to flat state. We analyze the vehicle speed histogram to take a closer look at behavior of vehicles with microscopic view in Fig. 5. There is only subtle difference between D-GWS(4, 4) case and D-GWS(36, 36) case. It indicates

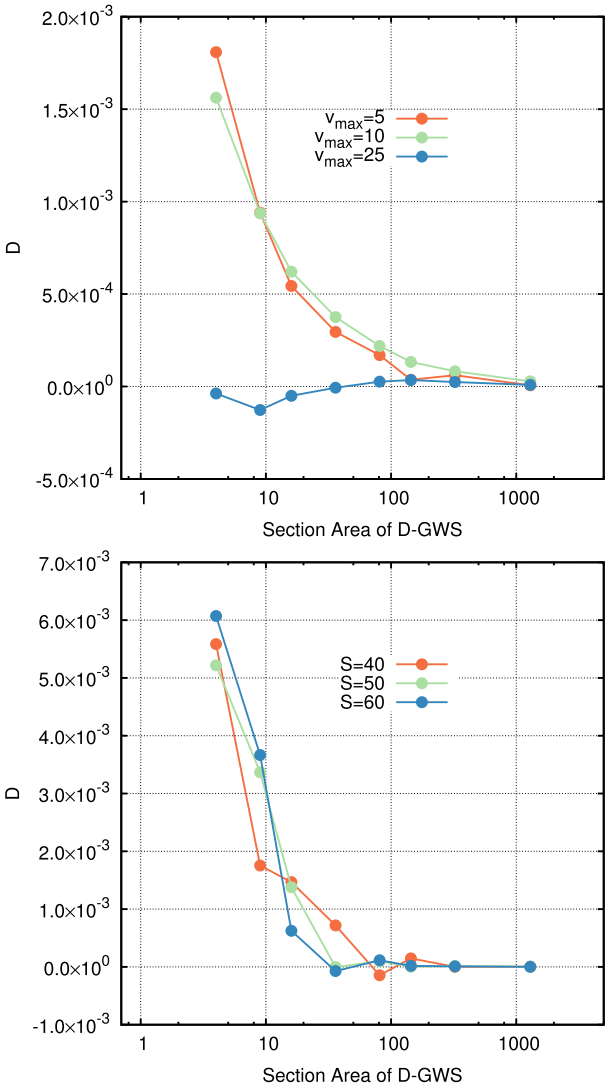

Fig. 6. Two variations of 36 × 36 GWS systems are presented to examine the alteration of critical point when two global parameters, maximum velocity $v_{\max}$ and street length L change. T_{delay} values for different global parameters are obtained from analytical calculation [1]. (top) Various maximum speeds $v_{\max} = 5, 10, 25$ are tested in GWS with $\rho = 0.03$. T_{delay} is 10, 5, and 2, respectively. With the increase in $v_{\max}$, the critical point moves to higher section area. The case of extremely high $v_{\max}$ shows that section area expansion makes no contribution to mean flow. (bottom) Various street lengths $L = 40, 50, 60$ are tested in GWS with $\rho = 0.7$. T_{delay} is -44, -55, and: -66, respectively. We check out that the critical point shifts from the fourth point to the fifth point in the case of shorter street length.

local congested states are decentralized independently. We are sure that D-GWS(4, 4) size is the specific size enough to unwrap the jam state. Therefore, the outbreak of crossover at D-GWS(4, 4) is an inevitable conclusion. From the argument, we can infer that the shift of critical point depends only on the global parameter, such as maximum velocity $v_{\max}$ and street length L. We analyze the critical point displacement for global parameter variation and show the results in the Fig. 6. It indicates that two global parameters can make movement of the critical point. Variation of two global parameters is under the rule of making the most outperformed GWS because we need to maintain the property of the original green wave strategy [1]. Exceptionally, phase transition phenomenon suddenly slips away at the case of $v_{\max} = 25$ ($\rho = 0.03$, $L = 50$). Maximum velocity 25 over street length 50 is very unrealistic (corresponds to 675 km/h). Also, it is not applied to analysis of D-GWS because the system is changed to one-shot game, namely, vehicle can escape the simulation map at one go. It is the rationale for disappearance of phase transition.

We show the snapshot of D in two stages: the early stage of the area extension and the late stage of the area extension. Fig. 7 includes the snapshot of (a) the early stage of the area extension and (b) the late stage of the area extension in the free-flow state ($\rho = 0.05$). Fig. 8 shows the snapshot of (a) the early stage of the area extension and (b) the late stage of the area extension in the jam state ($\rho = 0.7$). In Figs. 7 and 8, we conclude the existence of two phases in both cases, which

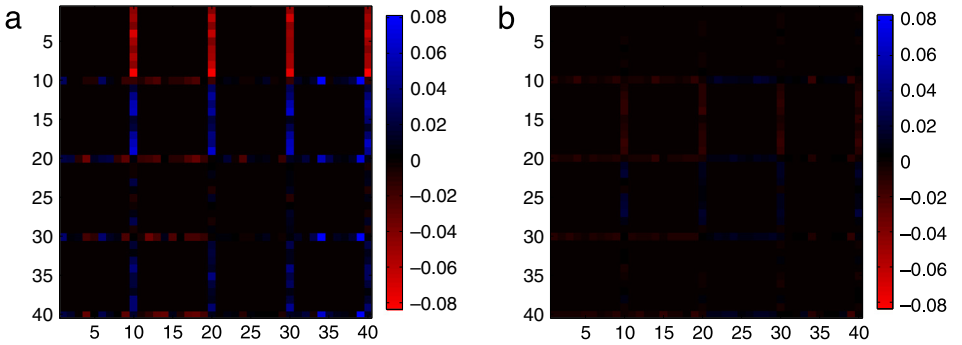

Fig. 7. Snapshot of 4 × 4 D-GWS for checking the effect of area extension in free-flow state. The picture (a) shows the early stage of area extension and displays the variation of the vehicle speed. The picture (b) shows the late stage of area extension and displays no change of the vehicle speed.

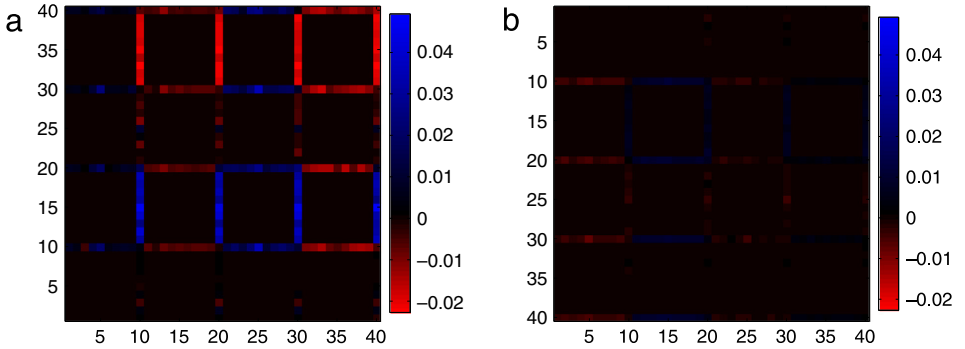

Fig. 8. Snapshot of 4 × 4 D-GWS for checking the effect of area extension in jam state. The picture (a) shows the early stage of area extension and displays the variation of the vehicle speed. The picture (b) shows the late stage of area extension and displays no change of the vehicle speed.

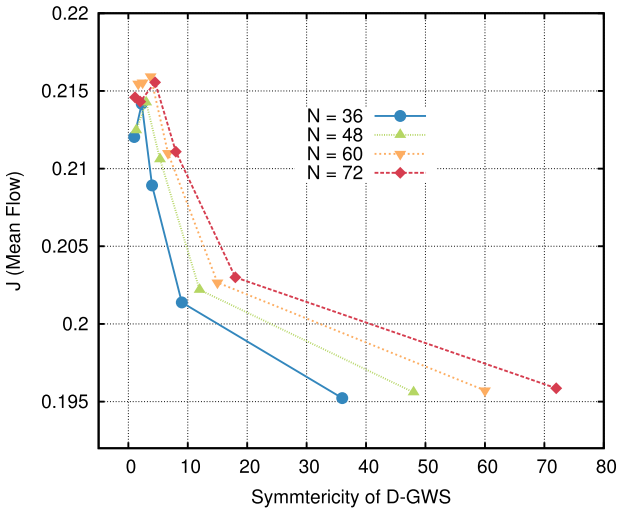

Fig. 9. Symmetricity S vs. mean flow J in map size 36, 48, 60, and 70. The relationship between two parameters is an inverse proportion. The graph indicates the low symmetricity, namely more squared form section, is more efficient to the traffic system.

actively changes the mean flow below the specific point of the section area, whereas no change in the mean flow occurs above the specific point.

3.2. Fixed section area with changing symmetricity

As previously mentioned, various cases include identical section areas. We have introduced the symmetricity, which is a type of aspect ratio of the rectangular pieces, to distinguish these pieces. In this section, we focus on the property of symmetricity and establish the relationship between the symmetricity and the mean flow J under the same area conditions.

Fig. 9 shows the relationship between symmetricity S and mean flow J with the fixed system size. For instance, the case of $N = 36$, five points on Fig. 9 indicates D-GWS(6, 6), D-GWS(9, 4), D-GWS(12, 3), D-GWS(18, 2), and D-GWS(36, 1), which symmetricity value of 1, 2.25, 4, 9, and 36, respectively. The results of Fig. 9 indicate that the symmetricity is inversely proportional to the mean flow. Although there is small fluctuation in the low value range, there is strictly inverse relationship between S and J. One can analyze the results for the magnitude of the symmetricity, which indicates that the higher the symmetricity value is, the longer the adjoining edge is, which causes the low J with a strong phase gap. This explanation demonstrates why the lowest symmetricity value, i.e., square formed section, yields the highest J. The square formed section encompasses the smallest perimeter with the given area. The fitted line is a curve with an inflection point instead of a distinct descending line; however, the difference in J is very small over the low S values. We have performed the same process using different D-GWS and observed the same tendency regardless of the map size. Consequently, J decreases according to the increase in the symmetricity value.

3.3. Comparison between empirical data and numerical simulation

A superior theory would have to reproduce the empirical findings equally well with fewer parameters to obtain a better quantitative agreement with the data using the same number of parameters or reproduce additional observations [5]. In this section, we attempt to compare the simulation results with the empirical data. The description of the data is as follows: (1) The monthly data for the average speed on urban arterial highways are supported by Seoul local government figures. (2) The data points range from January 2004 to June 2010. Data for 2007, March 2006, and May 2008 were excluded due to data loss. (3) The total number of data points for 25 districts and 64 months is 1600. The description of the data is detailed in Appendix C.

To exclude the irregular effect resulting from various conditions, such as weather, construction, and natural disasters, we average all data points for the vehicle speeds in each district. Each value of the area of the district is obtained from the government figures. However, we should calculate the area and symmetricity of each section for each district. Straight alignment of the rows is difficult, and there is no exact integer value due to the irregular shape of the sections. Thus, we use a polygon approximation. A complete explanation of the methods in our analysis is provided in Appendix C.

Using the findings from the empirical data, we plot two graphs: mean flow versus section area (Fig. 10) and mean flow versus symmetricity (Fig. 11). In addition, we add the simulation results in terms of the mean flow versus section area to facilitate the comparison with the empirical data (Fig. 4). From Fig. 4, the mean flow proceeds with near flat-line growth after the specific point of the section area, which indicates no contribution by the extension of the area to the mean flow, as observed in the graph of empirical data. We can predict the flatness because the empirical data is large enough to show nearly 0 value of D. We divide each sector by urban arterial highways, and each intersection is usually separated by 1 km or more. According to NS model [33,34], the length of a single cell is set to 7.5 m. The street of original toy model is consisted of 50 cells ($L = 50$), therefore total length of one district in simulation model is around 375 m. From the above calculation, we can check that the section of real world is greater than 3×3 section in the simulation. Thus, we infer that the flatness can be happened because the section area of the empirical data is near the critical value D-GWS(4, 4). The red fitting line tends to become flatter with an increase in the section area, especially toward the EP point.

In the previous section, we observed the effect of symmetricity on the simulation results of the mean flow, as shown in Fig. 9. We also obtain the inverse relationship between the mean flow and symmetricity in the empirical data graph, as shown in Fig. 11, especially from point GJ to point GB. An increase in the symmetricity value reduces the traffic efficiency, with a significant reduction in the mean flow. Therefore, we can conclude that two parameters the section area and the symmetricity play a significant role in improving the traffic efficiency in terms of the mean flow, which is supported by the numerical simulation and the empirical data analysis. Based on this finding, we must consider two important parameters when we study or design traffic systems.

Identical outliers are detected in the two graphs in Figs. 10 and 11: YS, DJ, GC GN and J. Points that stray from the average fitting line but follow the overall tendency are also observed. We analyze the points that are located too far from the line but that maintain the tendency of the entire set of data. As shown in Fig. 9, YD, MP and SD are large positive-deviated points. These three points generally exhibit low symmetricity value. Based on this low symmetricity value, the three points exhibit very high traffic efficiency and also maintain the properties of the graph. GA and GB indicate perfectly opposite phenomena because the two points exhibit high symmetricity value. We investigate why the outliers cannot follow the property of the other points. GN, YS and J are notorious for being chronically congested. GN always experiences heavy traffic due to overpopulation. YS and J lag behind other districts with respect to road conditions and also serve as transport centers. DJ and GC have no well-known characteristics of a traffic system. Thus, we can conjecture that the two districts utilize their own inherent properties to control the traffic efficiency. The explanation of this phenomenon is expected to attract various ideas that may reveal previously unknown important factors.

4. Conclusion

In this paper, we have investigated the effect of the divided GWS for the analogy to the bounded information accessibility problem in the real world. Each of the independent rectangular sections is representative of information restriction; thus, the

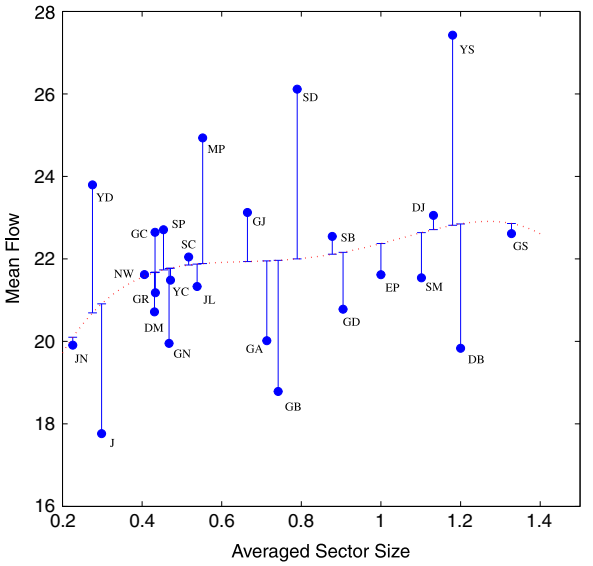

Fig. 10. Mean flow J vs. averaged section area of district in the empirical data. Before the curve reach the EP, the graph is prone to coincide with the simulation result (Fig. 9). After the point of EP, the graph is influenced by YS very effectively. YS is one of the representatives of irregular points. YS, DJ, GC, GN and J are outliers in the graph. YD, MP and SD are large positive deviate points and GA and GB are large negative deviate points due to the great effect of symmetricity. The fitting equation is $-28.562x^4 + 79.605x^3 - 83.348x^2 + 39.831x + 14.561$.

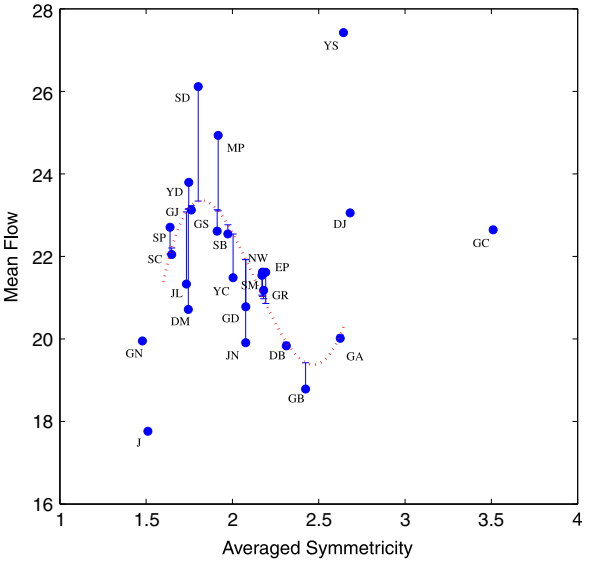

Fig. 11. Mean flow J vs. averaged symmetricity of district in the empirical data. We can observe the inverse relationship between two parameters easily in the range from GJ to GB. There are irregular behaviors with outer part of the GJ and GB, therefore, the graph is distorted with those deviations. The fitting equation is $-6.2762x^4 + 83.439x^3 - 362.37x^2 + 641.37x - 377.78$.

D-GWS is a more realistic model because it exhibits limited linkage due to costs and technical problems. The D-GWS has two main parameters, the section area and the symmetricity of the area resulting from the division property and the independent decentralized control system. Under the fixed symmetricity, the D-GWS shows two similar yet differing tendencies in terms of vehicle density. When the vehicle density is low, the phase gap of the traffic signals between individual sections is a more dominant factor than in the high-density case, which causes vehicles to stop. This allows the section area to be retained as a main factor until it expands to a critical value. Compared with low-density areas, the modified ChSch model in high-density areas exhibits a tendency to produce a clear phase transition. Therefore, we can analyze the clear phase transition phenomenon, which suggests a significant contribution to the mean flow with the interlocking effect in the early stage of area extension. However, it is meaningless to expand the section area above the critical point. In the D-GWS with a fixed section area, the symmetricity varies as a function of width and height. We have observed that the impact of the symmetricity for a fixed area creates an inverse proportional relationship between the symmetricity value and the rescaled

J. Low symmetricity value with a relatively lower perimeter causes an increase in J. The symmetricity becomes important in situations with locally high density regions. Although it only acts locally, the symmetricity can have a strong impact on global quantities such as flow.

Based on our research, we have determined that the empirical data correspond with the simulation results despite a few outliers. The results are reasonable because Seoul is one of the biggest cities in the world.

The D-GWS generates critical points due to the change in section area and symmetricity. It can lead to a compromise between efficiency and technical costs. Although the method cannot overcome the role of the pure GWS with respect to the mean flow due to the existence of the phase gap to reduce the mean flow, the D-GWS exhibits various effects in the sections resulting from changes in the section area and the symmetricity. We confirm that we can obtain sufficient mean flow when solving a traffic problem with a smaller section area compared with the original GWS and that the smallest symmetricity is optimal in terms of the efficiency of a traffic system. Our study considers the trade-off between efficiency and cost. When an urban planner designs city roads with limited resources, he or she should try to balance efficiency and technical limitations using section areas and symmetricity. Follow-up studies may demonstrate the need for the D-GWS to change from an independent decentralized version to a self-organized decentralized control system. By tracing the causes of abnormal behavior from the empirical data, another major factor of traffic efficiency can be determined.

Appendix A. Detailed model description

The velocity update rule of the modified ChSch model for nth vehicle is followed by Ref. [1]. :

Step 1: *Acceleration*

$$v_n \rightarrow \min(v_n + 1, v_{\max}). \tag{A.1}$$

Step 2: *Deceleration*

Case 1: The next traffic light is red for nth vehicle

$$v_n \rightarrow \min(v_n, d_n - 1, s_n - 1). \tag{A.2}$$

Case 2: The next traffic light is green for nth vehicle

If the next two cells directly behind the intersections are occupied

$$v_n \rightarrow \min(v_n, d_n - 1, s_n - 1), \tag{A.3}$$

Otherwise

$$v_n \rightarrow \min(v_n, d_n - 1). \tag{A.4}$$

Step 3: *Randomization with the probability p*

$$v_n \rightarrow \max(v_n - 1, 0). \tag{A.5}$$

Step 4: *Movement*

$$x_n \rightarrow x_n + v_n, \tag{A.6}$$

p is a randomization probability, x_n denotes the position of nth car, $d_n = x_{n+1} - x_n$, the distance to the next car and v_n represents the velocity of nth car. Finally, s_n indicates the distance between the traffic lights and nth car. The case 2 of step 2 makes a vehicle possible to occupy intersections if and only if it assumes that the vehicle leaves the intersection in the next step.

Appendix B. D-GWS in various density conditions

We try to figure out the property of D-GWS. First, we check out whether the extreme cases of the D-GWS have analogy with the original GWS. We can confirm that the expansion of D-GWS is same as the original GWS from Fig. B.1. Second, to demonstrate the preservation of the concept of the GWS, we try to test the offset effect on various density conditions, $\rho = 0.1$–0.9. Fig. B.2 shows the nine cases of the density from $\rho = 0.1$ to $\rho = 0.9$, respectably. From the results, we can conclude that offset parameter $T_{delay} = 10$ is the best in low density while offset parameter $T_{delay} = -55$ is the best in high density.

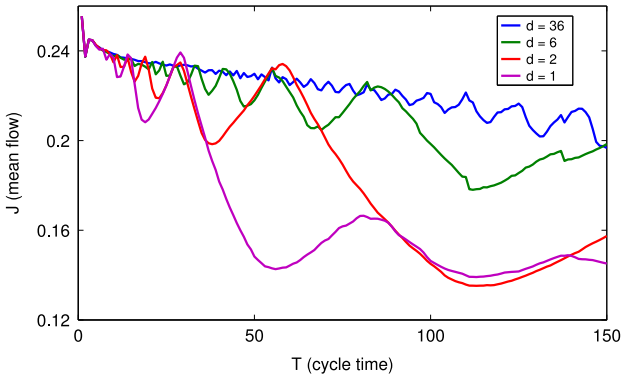

Fig. B.1. Mean flows J vs. cycle time T in 36 × 36 D-GWS. The character d means length of square division, thus each curve represents D-GWS(36, 36), D-GWS(6, 6), D-GWS(2, 2), and D-GWS(1, 1). D-GWS(36, 36) shows the same behavior as the 36 × 36 GWS in the Ref. [1], and D-GWS(1, 1) shows the same behavior as the perfectly synchronized state with one single intersection in the Ref. [1]. We set the random parameter as $p = 0.1$ and the density as $\rho = 0.7$.

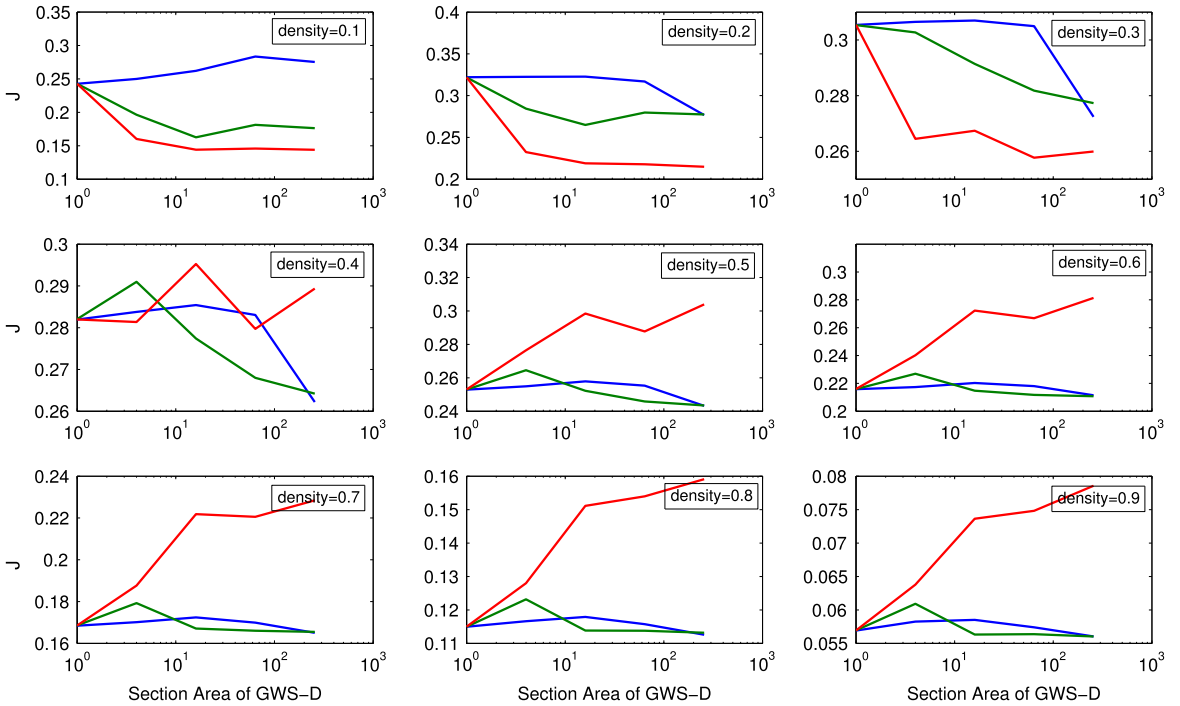

Fig. B.2. Mean flow J vs. section area of D-GWS on various density conditions. Each point on the line represents offset 10(blue), 30(green), and −55 (red) with respective section area. Regardless of the section area of D-GWS, there are dominant offsets in both low and high density, offset parameter $T_{delay} = 10$ and offset parameter $T_{delay} = -55$. (For interpretation of the references to color in this figure legend, the reader is referred to the web version of this article.)

Appendix C. Detailed empirical data analysis method

We consider average vehicle speed as the mean flow because the mean flow represents the amount of how well does vehicle go forward. We extract the data points from independently controlled 24 districts in Seoul, Korea. In Fig. C.1(b), we sketch the whole map of Seoul and mark the each district with designate, for example, 'GN' represents 'Gang-Nam'. Each district is governed by authority of autonomous district and is followed by 'Gu', for instance, 'GN' is called by 'Gang-Nam Gu'. There are also many independently functioning sections as to traffic in each district, which is depicted in Fig. C.1(a). The sections in each district is classified by urban arterial highways, given the fact that urban arterial road has only traffic lights at entry and exit gate and functions its role independently in Seoul [39].

To identify two main parameters, section area and symmetricity, we should calculate the area and symmetricity of all sections. It is impossible for street in the reality with simple calculation method given that almost of all shape of sections are irregular. The point leads mismatches between real world and the ideal numerical simulation. We use the concept of

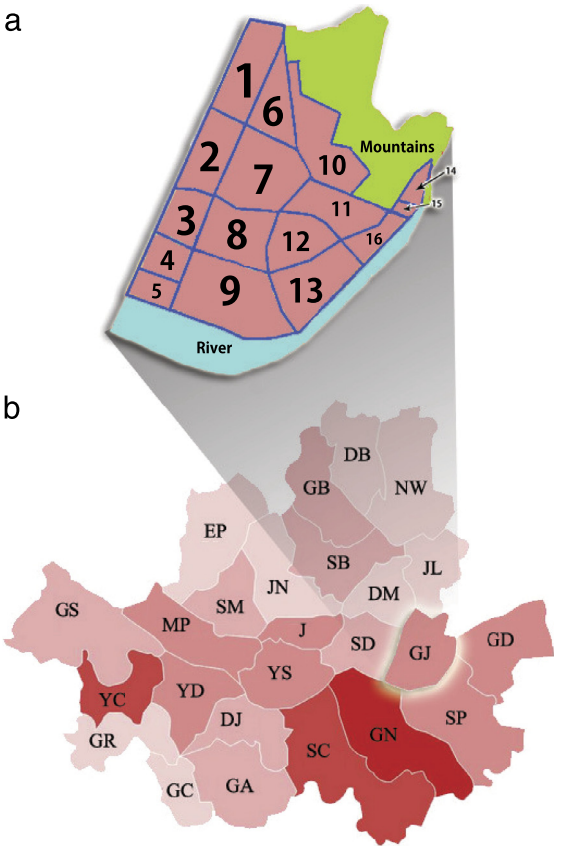

Fig. C.1. The figure shows the map of Seoul(b) and an example of GJ for separating the sections. Seoul is consisted of 24 independent districts which are controlled by authority of autonomous district. We set up the boundaries on each district according to urban arterial highways. If there are river and mountains in the district, they are excluded from the calculation.

Table C.1
The table includes statistics from the empirical data. Mean flow indicates that the average vehicle speed on the urban arterial highways in each district. Symmetricity is calculated by dividing longer side of the rectangular sector into shorter side. Sector size is averaged out with all sections in each district except for river and mountains, based on the boundaries of the urban arterial highways.

Number	District	Mean flow	Symmetricity	Sector size
1	J	17.76	1.510	0.298
2	GB	18.78	2.423	0.742
3	DB	19.83	2.311	1.200
4	JN	19.90	2.077	0.226
5	GN	19.95	1.478	0.468
6	GA	20.02	2.625	0.713
7	DM	20.72	1.744	0.431
8	GD	20.78	2.077	0.905
9	GR	21.18	2.180	0.433
10	JL	21.33	1.733	0.538
11	YC	21.49	2.004	0.471
12	SM	21.54	2.171	1.102
13	EP	21.62	2.193	1.000
14	NW	21.62	2.174	0.406
15	SC	22.05	1.648	0.517
16	SB	22.55	1.974	0.878
17	GS	22.61	1.912	1.328
18	GC	22.65	3.511	0.433
19	SP	22.70	1.638	0.454
20	DJ	23.06	2.682	1.132
21	GJ	23.13	1.762	0.665
22	YD	23.79	1.747	0.275
23	MP	24.93	1.917	0.552
24	SD	26.12	1.802	0.789

minimum bounding box to resolve the conflict [41]. Among various methods, we apply the elongatedness, which is ratio between the length and width of the region bounding rectangle [42]. The elongatedness serve as an extended concept of symmetricity. The process is following: First, we make the rectangle of minimum area that bounds the shape, which is located by turning in discrete steps until a minimum is located. Second, we measure a ratio between the length and width of the rectangle. The ratio is frequently used in various disciplines [43,44]. From Fig. C.1(a), we easily can check that there are various concave or convex polygonal region. Following the above mentioned process, we transform a concave polygon into a circumscribed quadrilateral. When we handle a convex polygon, the convex polygon is divided to two concave polygons. (See Table C.1.)

References

[1] E. Brockfeld, R. Barlovic, A. Schadschneider, M. Schreckenberg, Optimizing traffic lights in a cellular automaton model for city traffic, Phys. Rev. E 64 (5) (2001) 056132.
[2] D. Helbing, Traffic and Granular Flow'99 — Social, Traffic, and Granular Dynamics, Springer-Verlag, Berlin and Heidelberg, 2000.
[3] B.A. Toledo, V. Mu noz, J. Rogan, C. Tenreiro, J.A. Valdivia, Modeling traffic through a sequence of traffic lights, Phys. Rev. E 70 (1) (2004) 016107.
[4] I. Prigogine, R. Herman, Kinetic Theory of Vehicular Traffic, Elsevier, Amsterdam, 1971.
[5] D. Helbing, I. Farkas, T. Vicsek, Simulating dynamical features of escape panic, Nature 407 (6803) (2000) 487–490.
[6] W.J. Yu, R. Chen, L.Y. Dong, S.Q. Dai, Centrifugal force model for pedestrian dynamics, Phys. Rev. E 72 (2) (2005) 026112.
[7] S. Lammer, D. Helbing, Self-control of traffic lights and vehicle flows in urban road networks, J. Stat. Mech. Theory Exp. 2008 (04) (2008) P04019.
[8] Q.L. Li, R. Jiang, Z.J. Ding, J. Min, B.H. Wang, Effect of vehicles' changing lanes in the Biham–Middleton–Levine traffic flow model, Internat. J. Modern Phys. C 26 (03) (2015) 1550032.
[9] S. Boccaletti, et al., The structure and dynamics of multilayer networks, Phys. Rep. 544 (1) (2014) 1–122.
[10] Q.L. Li, B.H. Wang, M.R. Liu, An improved cellular automaton traffic model considering gap-dependent delay probability, Physica A 390 (7) (2011) 1356–1362.
[11] Q.L. Li, R. Jiang, B.H. Wang, M.R. Liu, Phase diagrams of traffic flow at an unsignalized intersection, Europhys. Lett. 99 (3) (2012) 38004.
[12] A. Kirchner, K. Nishinari, A. Schadschneider, Friction effects and clogging in a cellular automaton model for pedestrian dynamics, Phys. Rev. E 67 (5) (2003) 056122.
[13] V.J. Blue, J.L. Adler, in: A. Ceder (Ed.), Proceedings of the 14th International Symposium on Transportation and Traffic Theory, Pergamon, New York, 1999, pp. 235–254.
[14] V.J. Blue, J.L. Adler, Modelling four-directional pedestrian flows, Transp. Res. Rec. 1710 (1) (2000) 20–27.
[15] Q.L. Li, R. Jiang, J. Min, J.R. Xie, B.H. Wang, Phase diagrams of heterogeneous traffic flow at a single intersection in a deterministic Fukui-Ishibashi cellular automata traffic model, Europhys. Lett. 108 (2) (2014) 28001.
[16] A. Schadschneider, in: M. Schreckenberg, S.D. Sharma (Eds.), Pedestrian and Evacuation Dynamics, Springer, Berlin, 2002, pp. 75–77.
[17] D. Helbing, P. Molnar, Social force model for pedestrian dynamics, Phys. Rev. E 51 (5) (1995) 4282.
[18] D. Helbing, I.J. Farkas, P. Molnar, T. Vicsek, Simulation of pedestrian crowds in normal and evacuation situations, Pedestr. Evacuation Dyn. 21 (2002) 21–58.
[19] S. Okazaki, A study of pedestrian movement in architectural space. Part 2: Concentrated pedestrian movement, Trans. AI 284 (1979) 101110.
[20] T. Nagatani, Chaos and dynamical transition of a single vehicle induced by traffic light and speedup, Physica A 348 (2000) 561–571.
[21] Q.L. Li, B.H. Wang, M.R. Liu, Phase diagrams properties of the mixed traffic flow on a crossroad, Physica A 389 (21) (2010) 5045–5052.
[22] D. Helbing, A. Johansson, J. Mathiesen, M.H. Jensen, A. Hansen, Analytical approach to continuous and intermittent bottleneck flows, Phys. Rev. Lett. 97 (16) (2006) 168001.
[23] W.X. Wang, B.H. Wang, W.C. Zheng, C.Y. Yin, T. Zhou, Advanced information feedback in intelligent traffic systems, Phys. Rev. E 72 (6) (2005) 066702.
[24] Z.J. Ding, R. Jiang, B.H. Wang, Traffic flow in the Biham–Middleton–Levine model with random update rule, Phys. Rev. E 83 (4) (2011) 047101.
[25] Q.L. Li, R. Jiang, B.H. Wang, Emergence of bistable states and phase diagrams of traffic flow at an unsignalized intersection, Physica A 419 (2015) 349–355.
[26] Z.J. Ding, R. Jiang, M. Li, Q.L. Li, B.H. Wang, Effect of violating the traffic light rule in the Biham–Middleton–Levine traffic flow model, Europhys. Lett. 99 (6) (2012) 68002.
[27] J.R. Xie, R. Jiang, Z.J. Ding, Q.L. Li, B.H. Wang, Dynamical traffic light strategy in the Biham–Middleton–Levine model, Phys. Rev. E 87 (2) (2013) 022812.
[28] T. Nagatani, Control of vehicular traffic through a sequence of traffic lights positioned with disordered interval, Physica A 368 (2006) 560–566.
[29] S. Lammer, H. Kori, K. Peters, D. Helbing, Decentralised control of material or traffic flows in networks using phase-synchronisation, Physica A 363 (1) (2006) 39–47.
[30] D. Chowdhury, A. Schadschneider, Self-organization of traffic jams in cities: Effects of stochastic dynamics and signal periods, Phys. Rev. E 59 (2) (1999) R1311.
[31] A. Schadschneider, D. Chowdhury, E. Brockfeld, K. Klauck, L. Santen, J. Zittartz, Traffic and Granular Flow'99, Springer, New York, 2000.
[32] O. Biham, A.A. Middleton, D. Levine, Self-organization and a dynamical transition in traffic-flow models, Phys. Rev. A 46 (10) (1992) R6124.
[33] K. Nagel, M. Schreckenberg, A cellular automaton model for freeway traffic, J. Phys. I 2 (12) (1992) 2221–2229.
[34] N. Jia, S. Ma, Traffic-light boundary in the deterministic Nagel–Schreckenberg model, Phys. Rev. E 83 (6) (2011) 061150.
[35] K.H. Chung, P.M. Hui, G.Q. Gu, Two-dimensional traffic flow problems with faulty traffic lights, Phys. Rev. E 51 (1) (1995) 772.
[36] D.W. Huang, W.N. Huang, Traffic signal synchronization, Phys. Rev. E 67 (5) (2003) 056124.
[37] S.B. Cools, C. Gershenson, B. D0Hooghe, Self-organizing traffic lights: A realistic simulation, in: M. Prokopenko (Ed.), Advances in Applied Self-Organizing Systems, Springer, New York, 2007.
[38] M.E. Fouladvand, M. Nematollahi, Optimization of green-times at an isolated urban crossroads, Eur. Phys. J. B 22 (3) (2001) 395–401.
[39] J.T. Kim, et al., Transportation technology and policy 3 (2006) 190–201.
[40] M. Horyski, Intelligent electric systems in urban traffic control, in: Teka Komisji Motoryzacji i Energetyki Rolnictwa, in: Commission Motorization and Power Industry in Agriculture, vol. 7, 2007, pp. 110–115.
[41] H. Freeman, R. Shapira, Determining the minimum-area encasing rectangle for an arbitrary closed curve, Commun. ACM 18 (7) (1975) 409–413.
[42] M. Sonka, V. Hlavac, R. Boyle, Image Processing, Analysis, and Machine Vision, Chapman & Hall, London, 1993, pp. 228–279.
[43] Y. Choo, B. Kang, Extraction of sizes and velocities of spray droplets by optical imaging method, KSME Int. J. 18 (7) (2004) 1236–1245.
[44] N. Varachiu, A fuzzy shapes characterization for robotics, in: Computational Intelligence, Springer, Berlin Heidelberg, 1999, pp. 253–258.